2×1 reconstructed Si(111) surface: STM experiments versus *ab initio* calculations

J. K. Garleff, M. Wenderoth,* K. Sauthoff, and R. G. Ulbrich
IV. Physikalisches Institut der Universität Göttingen, Tammannstrasse 1, 37077 Göttingen, Germany

M. Rohlfing
School of Engineering and Science, International University Bremen, P.O. Box 750561, 28725 Bremen, Germany
(Received 8 June 2004; published 21 December 2004)

The electronic structure of the Si(111)-2×1 surface has been studied with scanning tunneling spectroscopy (STS). A large experimental local density of states data set of LDOS(x,y,E) with subatomic resolution has been compared with *ab initio* calculated LDOS distributions. The influence of the tunneling tip DOS has been eliminated by repeated measurements with different tips. The experimentally determined shape of the LDOS(x,y,E) agrees very well with the calculated results based on the π-bonded-chain model for both the surface valence and the conduction band. The good agreement with *ab initio* calculations of the electronic structure of the Si(111)-2×1 surface shows that STS provides reliable information of the sample LDOS even with subatomic resolution.

DOI: 10.1103/PhysRevB.70.245424 PACS number(s): 68.37.Ef, 73.20.At

I. INTRODUCTION

Scanning tunneling microscopy (STM) is a near field method that gives atomic resolution on most semiconductor surfaces. Dangling bonds located above each top layer atom of semiconductor surfaces can easily be addressed with the tunneling tip.[1] This in contrast to metal surfaces, where the weakly corrugated electron gas density contains much less information about the underlying lattice. In the constant current STM mode, all states in the energy range between the Fermi levels of the tip E_F and the sample (E_F+eV_{sample}) contribute to the tunneling current. In past years, intense efforts have been undertaken to explore energy-resolved spectra of the electronic surface structure. Recent atomic force microscopy (AFM) experiments mapped single bonds in the Si(111)-7×7 surface,[2] although details of the theoretical interpretation of this more elaborate method are still under discussion.[3] On the other hand, STM including its various extensions has become an experimental technique with a well established theoretical background (e.g., Ref. 1 and refs. therein). Voltage-dependent corrugation patterns were reported on cleaved GaAs(110)-surfaces in STM topographies with interlaced lines at different sample voltages (multibias mode). They were explained by addressing different surface resonances with the tunnel current[4] at distinct sample voltages. With current imaging tunneling spectroscopy (CITS) Hamers *et al.*[5] imaged the electronic structure of the Si(111)-7×7 surface within the surface unit cell ($\sim 2.7\times 2.7$ nm^2). Their spatial resolution was ~3 Å, the energetical resolution ~100 meV between −2 V and +2 V.

In this paper we present an experimental study of spatially resolved STS measurements at $T=8$ K on *in situ* cleaved Si(111) samples and a comparison with *ab initio* calculations of the electronic structure of the 2×1 reconstruction. As a function of the applied sample voltage in the range $-2\text{ V} < V_{\text{sample}} < 2\text{ V}$ we present here highly resolved local density of states (LDOS) distributions inside the unit cell. Local spectroscopic information on a subatomic scale necessarily is a convolution between sample and tip. The features that reproducibly occur in repeated measurements with several tips originate most likely from the LDOS of the sample. Our data confirm and considerably expand well known experimental results.[6] The observed characteristic variations of the LDOS(x,y,E) are in excellent agreement with the calculations based on the π-bonded-chain model proposed by Pandey.[7] The good agreement with *ab initio* calculations of the electronic structure of the Si(111)-2×1 surface shows that STS provides reliable information of the sample LDOS even with subatomic resolution.

II. EXPERIMENTAL SETUP

Atomically flat and clean Si(111) surfaces were prepared by *in situ* UHV cleavage along the $[\bar{2}11]$ direction of *n*-type Si crystals doped with 6×10^{18} phosphorous atoms per cm^3 at room temperature. The cleaved samples exhibited the 2×1 reconstruction and were transferred into the precooled STM. They reached the equilibrium temperature of 8 K, within less than an hour after cleavage. The experiments were done in a home built Besocke-type STM operating in UHV at a base pressure better than 5×10^{-11} mbar. The low-temperature system had a lateral drift of less than 0.5 Å/h. This offers sufficient mechanical stability over more than 4 h, which is necessary for high-resolution $I(V)$ spectroscopy. Our tips were electrochemically etched from polycrystalline tungsten wire. Further processing was done in UHV ($p_0 < 5\times 10^{-10}$ mbar) by glowing, sputtering, and characterization with field emission before transferring the tip into the STM. This treatment results in reproducible, highly stable tips that show no modifications of the apex atom for several hours.[8] The stability of the tips is a crucial point for high-quality laterally resolved $I(V)$ spectroscopy. The $I(V)$ spectroscopy was done in the range from −2.0 V to +2.0 V in steps of 40 meV. $I(V)$ was taken simultaneously with atomically resolved constant current images $Z(x,y)$ and the appar-

ent barrier height $\Phi(x,y)$. At this point one has to be aware that the experimental LDOS maps are recorded on a surface of constant current corrugated by about 1 Å while the theoretical LDOS(x,y) is presented on a plane of constant height. Assuming an exponential decay of the current with increasing tip-surface distance we project the experimental spectra by means of the measured $Z(x,y)$ and $\Phi(x,y)$ on a plane of constant height. We then interpret the $dI/dV(x,y)$ data (maps) at constant energy, which are extracted by numerical differentiation of the smoothed and projected $I(x,y,V)$, as the local variation of the LDOS(x,y,E). Numerical processing is done using gliding median and cubic-spline algorithms. After all numerics the energetical resolution is $\sim$100 meV and the lateral resolution is 0.25 Å.

Further improvement of the signal-to-noise ratio was achieved by averaging data of corresponding positions inside many unit cells. To create a template we fitted a global rectangular two-dimensional (2D) lattice to the visible periodicity in the LDOS maps and averaged over the data points on equivalent positions relative to this lattice. All discussed effects are observed in the raw data as well; the template technique included $\sim$600 unit cells and served here to improve the signal-to-noise-ratio.

As mentioned above, the measured spectra necessarily mix up information belonging to the electronic structure of the sample *and* the tip, especially if high spectral and lateral resolution is concerned. To circumvent this problem one can use blunt tips with an assumed constant DOS for the spectroscopy, but these tips reduce the lateral resolution. We tackle the problem of deconvolution of sample LDOS and tip influence on the spectra by repeating the measurements with several different tips and discuss here only those results that are reproduced for all of them. The above mentioned tip modifications improve the statistics, because each microstructure of the tip apex has a modified DOS. The analysis of this paper is based on about 20 data sets taken on 10 different samples with more than 10 different tips.

For a direct comparison with the experiments, we have carried out *ab initio* calculations of the surface, employing a combination of density-functional theory (DFT) and many-body perturbation theory (MBPT). Within DFT evaluated in the local-density approximation, using norm-conserving *ab initio* pseudopotentials and a basis of atom-centered Gaussian orbitals, the geometric structure of the Pandey-chain reconstruction is evaluated via total-energy minimization.

This is carried out by using a supercell configuration with a slab of 8 atomic layers, with one surface being passivated by hydrogen atoms. Employing 24 **k** points within the surface Brillouin zone, the atoms are relaxed until all forces are smaller than 0.001 Ry/a.u., and the remaining numerical error in the total energy is smaller than $\sim$0.004 eV per surface unit cell.

One particular issue concerns the orientation of the buckling of the Pandey chain, which can be either positive or negative (chain-right/chain-left isomerization).[9,10] Since the difference between the two orientations is only in the fourth atomic layer, it is extremely difficult to distinguish experimentally between them. Within the local density approximation (LDA), the energetic difference between the two orientations is very small; in fact, the chain with negative buckling (left chain) is preferred by 0.012 eV per surface unit cell (0.010 eV in Ref. 10). Nonetheless, we believe that the positively buckled chain (right chain) is more realistic because it leads to a quasiparticle gap energy (0.7 eV) and surface exciton energy (0.45 eV) in much better agreement with experimental data than the negatively buckled chain (cf. the discussion in Ref. 9). The latter yields a gap energy which is 0.2 eV lower. Note that the difference in total energy between the two configurations is very small. LDA, being an approximative method at its heart, may simply be not accurate enough to unambigously determine the more stable configuration. Furthermore, the preparation of Si(111)-2×1 itself (i.e., cleaving) might lead to the preference of the positively buckled chain although the negatively buckled chain may be lower in energy; after all, both are unstable relative to the Si(111)-7×7 reconstruction. At this point we focus on the positively buckled chain (chain-right configuration) due to its more realistic electronic spectrum.

A top view of the Pandey-chain structure is shown in Fig. 1(a), together with the resulting band structure in Fig. 1(b). The chain (running from the left to the right) is given by atoms 1 and 2; atoms 3 and 4 are in the subsurface layer, which is 1.0 Å lower in height than the Pandey-chain atoms. The optimized geometry is characterized by significant buckling, i.e., the atoms within the zigzaglike Pandey chain have alternating height, with a height difference of 0.51 Å between the "up" atoms [labeled 1 in Fig. 1(a)] and the "down" atoms [labeled 2 in Fig. 1(a)]. Due to the reduced coordination of the chain atoms that have threefold instead of the tetrahedrally fourfold coordination of the bulk, two dangling-bond states show up in the surface band structure [see Fig. 1(b)]. The accurate evaluation of the band-structure energies is not possible within DFT, but requires to include quasiparticle (QP) corrections that originate from exchange and correlation effects among the electrons. This is commonly done within the *GW* approximation (GWA) of the electron self-energy operator (see, e.g., Ref. 11). This approach has been shown to yield highly reliable band-structure data for a large variety of systems, with remaining uncertainties of less than 0.1 eV. In the present system, QP corrections are relevant both for the absolute value of the fundamental surface gap (0.7 eV in GWA as compared to 0.4 eV in DFT-LDA, only) and for the position of the surface bands relative to the bulk states. The πC_{VB} state, formed from p_z like orbitals at the up atoms, is lower in energy than the πC_{CB} state, which is mainly formed from p_z like orbitals at the down atoms. Consequently, the πC_{VB} band is filled, while the πC_{CB} band is empty. This constitutes a semiconducting band structure with a fundamental surface band gap of 0.7 eV. The band-structure data shown in Fig. 1(b) are in excellent agreement with experimental data from photoelectron spectroscopy (cf. Refs. 12 and 13). The electronic structure of the surface exhibits three features that will be of central importance for the STM data discussed below.

First, the tunneling current for energies near the gap will be dominated by the dangling-bond states instead of bulklike states near the Γ point, that are often considered as being most important for tunneling.[14]

Second, the lateral image of the tunneling current will be completely different below and above the gap, because it will

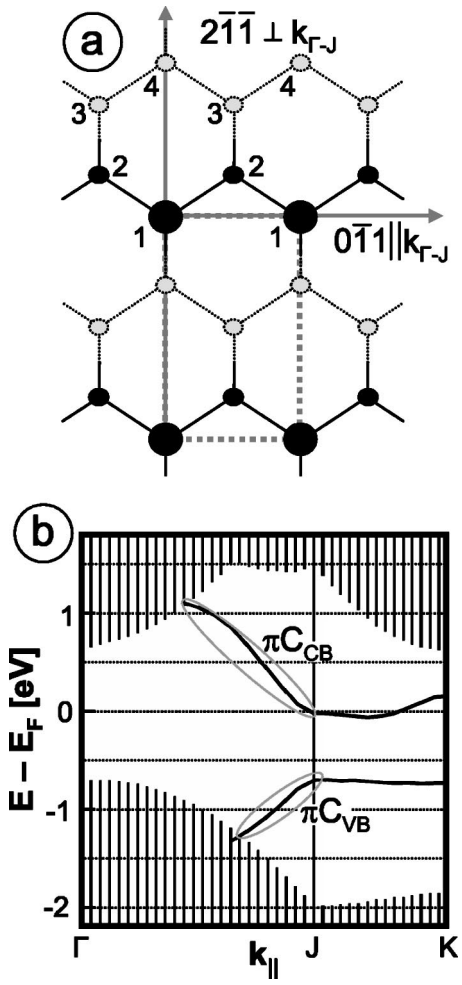

FIG. 1. Pandey model of the 2×1-reconstruction on Si(111). (a) Sketched top view of the (111) surface with numbers denoting different atom positions in the surface: 1, up atoms; 2, down atoms in the π-bonded chains; 3 and 4, atoms in the second layer row in between. The dotted line shows the 2×1 unit cell (6.65×3.84 Å^2). The real space lattice vectors correspond to the directions in k space as marked in the image. The crystallographic orientation with $[0\bar{1}1]$ along the x axis and $[\bar{2}11]$ along the y axis will be maintained in all following figures. (b) Calculated electronic surface dispersion with dangling bond states (black lines) and projected volume bands (hatched areas); πC denotes the π-chain states; the indices CB and VB denote states of conduction- and valence-band type.

originate from two states, πC_{VB} and πC_{CB} respectively, that are located at different atoms.

Third, it should be noted that the states which constitute the gap edges are located at the boundary of the surface Brillouin zone (along the *JK* line). This causes a sign change of the wave functions from unit cell to unit cell along the chain direction, leading to a nodal plane in between. It will lead to a very high contrast of the STM images at the gap edges since the tunneling current must vanish when these planes are crossed (see below).

The evaluation of the LDOS at selected energies as discussed below is done for a height of 5 Å above the surface. At this height, however, the amplitude of the Gaussian-orbital basis functions (having a radial behavior as $\exp[-\alpha r^2]$) is already extremely low and cannot be used to calculate the LDOS. Instead, we evaluate the wave functions $\psi_{n\mathbf{k}}(\mathbf{r})$ in a plane z_0 of just a few Å above the surface, i.e., where the Gaussians are still reliable and the potential has already decayed significantly. In this plane, we expand the wave function in two-dimensional plane waves, $\psi_{\mathbf{G}}(z)\cdot\exp[i(\mathbf{k}+\mathbf{G})\mathbf{r}_{\|}]$. The Schrödinger equation implies that each of these components $\psi_{\mathbf{G}}(z)$ will decay exponentially into the vacuum region beyond this plane as $\exp[-\kappa(z-z_0)]$ with a decay constant of $\kappa^2=(\mathbf{k}+\mathbf{G})^2+2m/\hbar^2\cdot(E_{\mathrm{vac}}-E_{n\mathbf{k}})$. This allows us to construct the wave function at any height z above the surface and to discuss the resulting STM features.

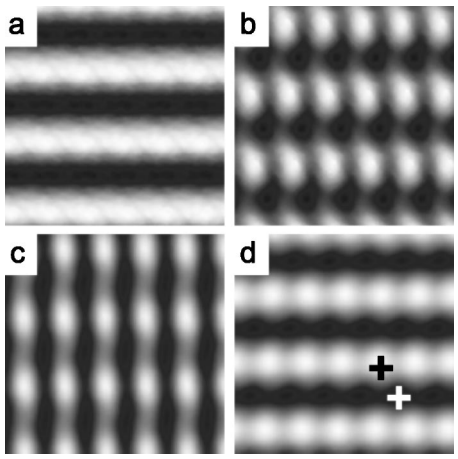

FIG. 2. Constant current images of (45×45 Å^2) on Si(111)-2×1 at different set points: +1.4 V; 0.5 nA (a), +0.6 V; 0.5nA (b), −0.3 V; 0.1 nA (c) and −1.1 V; 0.2 nA (d). Gray scaled with black, denoting minimal, and white, denoting maximal, tip height (the z range varies between the images). The black (white) cross marks the maximum (minimum) position as referred to in Fig. 3(b).

An important issue for the interpretation of STS data on semiconductors is the link between the control parameter V_{sample} in the experiment and the definition of the single electron energy E in the calculated surface band structure. Especially on (110) surfaces of III-V semiconductors tip induced band bending causes a complicated dependence of E on V_{sample}.[15] However, the Fermi level E_F on the Si(111)-2×1 surface is pinned in the fundamental gap of the volume band structure by the surface states,[16] and the applied voltage corresponds directly to the single electron energy scale: $eV_{\mathrm{sample}}=E-E_F$. Due to the high doping level of 6×10^{18} cm^{-3}, E_F is located slightly above the onset of the surface conduction band.

III. EXPERIMENTAL RESULTS

Figures 2(a)–2(d) show constant current topographies of defect free areas on the reconstructed Si(111) surface at several sample voltages from $V_{\mathrm{sample}}=+1.8$ to -1.2 V. At high voltages [Figs. 2(a) and 2(d)] the images are dominated by reconstruction lines in $[0\bar{1}1]$ direction. Going to smaller voltages a perpendicular corrugation in the $[\bar{2}11]$ direction

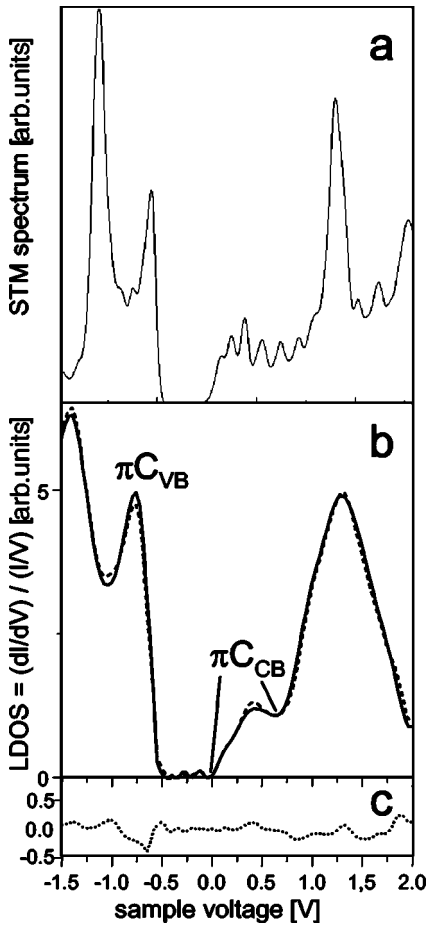

FIG. 3. LDOS on Si(111)-2×1 (a) *ab initio* calculated DOS(E) and (b) experimental spectra taken on (solid line) and between (dashed line) the maxima of the corresponding topography. Examples for both positions are marked in Fig. 2(d). The curves coincide expect for small differencies. (c) The difference between the dashed and the solid LDOS curve from subset (b) is plotted in the same scale and highlights the small variation inside the unit cell.

emerges; at a medium voltage of 0.6 V [Fig. 2(b)] the atomic corrugation in the $[\bar{2}11]$ as well as in the $[0\bar{1}1]$ direction is observed. Close to E_F at $E-E_F=-0.4$ eV [Fig. 2(c)] the $[\bar{2}11]$ direction dominates the visible corrugation.

In Fig. 3 we compare theoretically calculated (subset a) and experimentally measured (subset b) LDOS-spectra of the 2×1-reconstructed Si(111) surface. In both subsets the corresponding peaks have similar relative strength. For the experimental LDOS(E) we give two examples at different positions relative to the atomic lattice in Fig. 3(b): The solid and the dashed line show the LDOS(E) on the maxima and on the minima of the corresponding topography. The positions are marked by the black and the white cross in Fig. 2(d). The local variation within the surface unit cell turns out to be small. In Fig. 3(c) we plot the difference between both experimental LDOS(E) curves from subset b. Repeated measurements show that these small variations are significant and reproducible.

A comparison between experimentally determined and *ab initio* calculated locally resolved LDOS(x,y) can be seen in

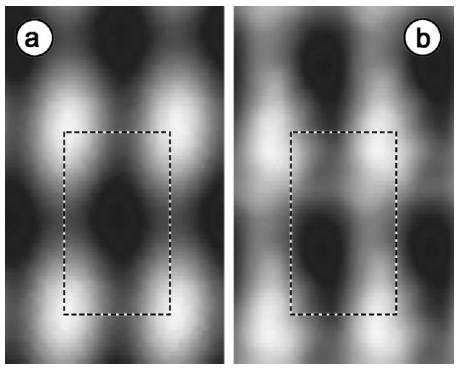

FIG. 4. (a) Constant current topography $Z(x,y)$ at $V_{sample}=-1.0$ V and $I_T=0.4$ nA and (b) apparent work function $\Phi(x,y)$ taken simultaneously. The corrugation amplitude $Z(x,y)$ due to the reconstruction pattern is about 1 Å. $\Phi(x,y)$ is modulated within the surface unit cell between 180 meV and 350 meV. The data are gray-scaled; light indicates high and dark indicates low values of Φ and $Z(x,y)$. Referring to the text and Fig. 5 we present a surface unit cell at the up atoms by the dashed rectangle. For crystallographic orientations see Fig. 1(a).

Figs. 5–7. For clarity in each figure the experimental data are called subset e_i (experiment), the corresponding calculated LDOS maps subset t_i (theory). The exponential decay of the tunneling current with increasing tip-sample distance Z is given by $I(Z,\Phi)\propto I_0 e^{-Z\lambda\sqrt{\Phi}}$ with $\lambda=\sqrt{8m\hbar^{-2}}$ and the apparent work function Φ. Simultaneously to the spectroscopy $I(x,y,U)$ the topography $Z(x,y)$ and $\Phi(x,y)$ was recorded (see Fig. 4). We multiply the measured $I(x,y,U)$ with the factor $e^{+Z(x,y)\lambda\sqrt{\Phi(x,y)}}$ to project the experimental data on a flat plane parallel to the surface. This projection allows direct comparison with theory. We divide the discussion of LDOS(x,y,E) as a function of energy in three parts. (i) We find best agreement between theory and experiment in the empty states probed at positive samples voltages: Above 1 V we observe a high total density of states with only small relative lateral variations as shown in Fig. 5 e_1. The LDOS maxima are not very pronounced and match roughly the theoretically predicted shape as rows along the up atoms of the π-bonded chains (Fig. 5 t_1). Below 1 V the contrast of the LDOS is higher. The LDOS maxima can be aligned with the theoretically expected positions close to the up atoms (Fig. 5 e_2,t_2). The method to locate the atomic nuclei relative to the STM data is discussed below. According to the calculations the LDOS maxima of the conduction-band states shift from the up atoms (above $E_F+0.6$ eV) to the down atoms (below $E_F+0.2$ eV; see Fig. 5 e_3,t_3). The transition region in the conduction band shows laterally broadened LDOS distributions covering the up and down atoms. (ii) Near the band onsets we observe a LDOS modulation along the $[0\bar{1}1]$ and $[\bar{2}11]$ direction. When switching across the fundamental surface band gap from $U_{sample}=+0.1$ V to $U_{sample}=-0.7$ V the LDOS maxima shift from the down atom about 1.9 Å in the $[0\bar{1}1]$ direction and about 1.5 Å in the $[\bar{2}11]$ direction (Fig. 6 e_1,e_2) to the up atom. (iii) For all negative voltages the LDOS maxima are expected close to the up atoms. The corrugation along the π-bonded chains is large for small nega-

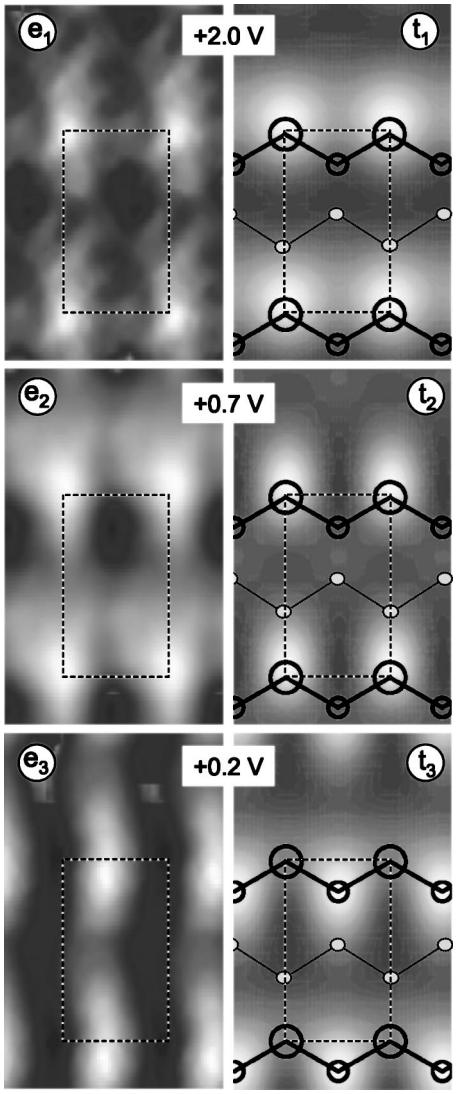

FIG. 5. Laterally resolved LDOS structure LDOS(x,y) of the empty states from theory (right, t_i) and experiment (left, e_i) at typical energies (white, high LDOS; black, low LDOS). In the calculated images the underlying atomic lattice is shown by large (small) open circles marking the up (down) atoms of the π-bonded chains and the gray filled circles marking the zigzag rows in between. The different surface atoms are referred to as numbers 1 to 4 in Fig. 1(a). We present a surface unit cell connecting at the up atoms (dashed rectangle). The characteristical shifts of the LDOS maxima relative to the atom positions is discussed in the text. For crystallographic orientations see Fig. 1(a).

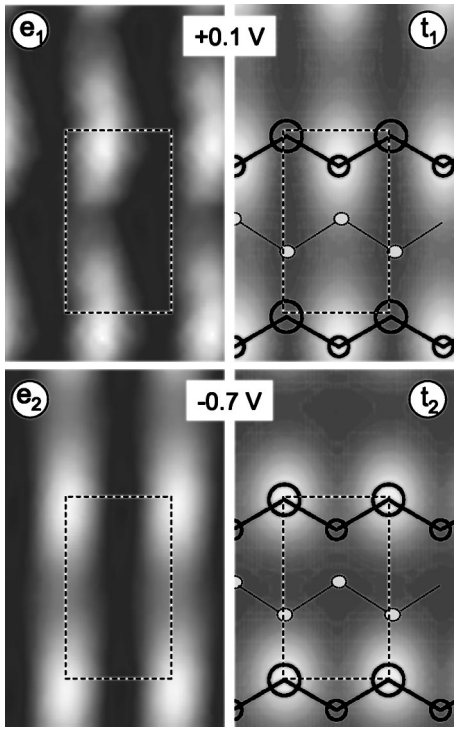

FIG. 6. LDOS(x,y) at the band onsets from experimental (left, e_i) and calculated (right, t_i) data. The LDOS maxima characteristically shift relative to the surface unit cell when the energy is switched from $\pi C_{\mathrm{VB}}(\mathrm{e}_1,\mathrm{t}_1)$ to $\pi C_{\mathrm{CB}}(\mathrm{e}_2,\mathrm{t}_2)$. For crystallographic orientations see Fig. 1(a); lattice positions and gray scale, see Fig. 5.

tive energies (Fig. 7 $\mathrm{e}_1,\mathrm{t}_1$) and decreases to higher negative energies (Fig. 7 $\mathrm{e}_2,\mathrm{t}_2$). Similar to the empty-state behavior, the LDOS patterns of the occupied states show a large contrast between E_F and $E_F-1.0$ eV (Fig. 7 e_1) and become blurred at lower energies. Far away from E_F the occupied states show a behavior similar to the empty states: a high LDOS with small corrugation (Fig. 7 e_2).

The topography images at several V_{sample} in Fig. 2(a)–2(d) can be understood as a superposition of the above-mentioned spectroscopic features. The well known 6.65 Å spaced lines in $[0\bar{1}1]$ direction[6] at high $|V_{\mathrm{sample}}|$ reflect the different geometrical height of the atoms 1 and 2 forming the π-bonded chains relative to atoms 3 and 4, as labeled in Fig. 1(a). This is in good agreement with the predicted height difference of 1 Å (see above). The pattern smoothly transforms from the above-mentioned lines into perpendicular rows of elliptical bonds at voltages close to E_F due to the electronic structure of the π-bonded chains.

STM in principle only maps the electronic structure of the surface. Without further assumptions it is not possible to determine the positions of the atomic nuclei. According to the calculations, the lowest empty states (Fig. 6 t_1) are located at the down atoms [see Fig. 1(a)]. The highest occupied state is located at the up atom (Fig. 6 t_2). The electronic surface structure from *ab initio* calculated theory and the measured LDOS spectra agree very well. The LDOS(x,y) was used to define the position of the underlying atomic lattice relative to the experimental LDOS distribution: We fix the positions of the atomic nuclei relative to the experimental STS images by comparing the experimental (Fig. 6) data and the calculations (Fig. 6) at $E-E_F=-0.7$ eV and $E-E_F=+0.1$ eV of the electron density on the surface. The LDOS maxima of these two energies indicate the dangling bonds at the up atom and the down atom, respectively. We chose a surface unit cell that connects the up atoms in all LDOS maps and fix it at the experimental LDOS maxima at $E-E_F=-0.7$ eV. This choice achieves a reasonable link between experiment and theory within the investigated energy range. Especially a second characteristic shift of the LDOS maxima between $E-E_F=$

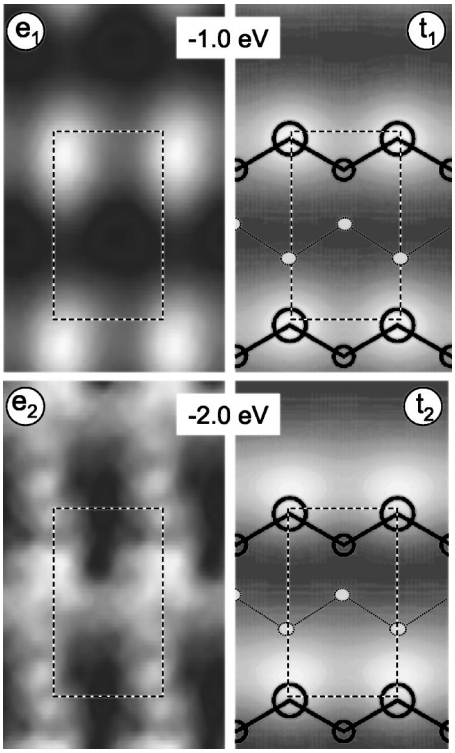

FIG. 7. Comparison of experimentally measured (left, e_i) and calculated (right, t_i) LDOS distributions in the occupied states. At high negative energies the structure fades out. For crystallographic orientations, see Fig. 1(a); lattice positions and gray-scale, see Fig. 5.

+0.7 eV and $E-E_F=+0.2$ eV in the empty states is found in theory as well as in the experiments (Fig. 5 e_1, e_2, t_1, t_2). The discrepancies between experiment and theory at high negative energies (Fig 7 e_2, t_2) are not surprising, because a detailed analysis of the tunneling process through the vacuum barrier showed earlier that the spectra contain less information about the sample LDOS at higher negative sample voltages.[17] The shift in the LDOS maxima when crossing the surface band gap [observation (ii)] is predicted quantitatively by the model. This shift can be seen in Fig. 6 for experiment and theory from e_1, t_1 to e_2, t_2. The calculations explain the strong corrugation along the rows: The states at the surface band edges are found near the *J* point in the reciprocal space; their wave functions change sign with each lattice constant along the π chain. So in the middle between two up atoms in the chain the πC_{VB} wave function has a node and the charge density vanishes; this behavior persists even several Å above the surface, where the tip probes the LDOS. The same holds for the πC_{CB} wave function, which has a node between two down atoms. These minima in the LDOS explain the $[\bar{2}11]$ corrugation along the chains.

The corrugation observed in the topographies in Fig. 2 rotates from $[\bar{2}11]$-direction [Fig. 2(c)] close to $V_{\mathrm{sample}}=0$ V to the $[0\bar{1}1]$ direction at higher voltages [Figs. 2(a) and 2(d)]. Theory describes this behavior also very well: The DOS increases with energetic distance from the band onsets. In the constant current mode at higher voltages the wave functions with small wave vectors deep inside the bands contribute more than the corrugation along $[\bar{2}11]$ introduced by the wave functions close to band onsets that are located near the zone boundary in reciprocal space.

In summary we presented an experimental study of STM and STS data combined with *ab initio* calculations of the electronic structure of the Si(111)-2×1 surface unit cell. The STM and STS measurements on *in situ* cleaved Si(111) samples investigate the electronic structure of the 2×1 reconstruction in detail within the surface unit cell at 8 K. The dominant effects are (1) a characteristic LDOS shift between the up and the down atom when crossing the surface band gap, (2) a similar shift inside the empty surface state band with a transition region around $E-E_F=+0.4$ eV, and (3) a transition to dominating $[\bar{2}11]$-orientated corrugation close to the band edges. All three observations are well described by *ab initio* theory based on the π-bonded-chain model. Repeated measurements with several different tips allowed to deconvolute the tip effects from the electronic structure of the sample: Features that were reproduced with all tips gave reliable (x,y,E) maps of the sample LDOS with subatomic resolution.

*Electronic address: wendero@ph4.physik.uni-goettingen.de

[1] C. J. Chen, *Introduction to Scanning Tunneling Microscopy* (Oxford University Press, Oxford, 1993).
[2] F. J. Giessibl, S. Hembacher, H. Bielefeldt, and J. Mannhart, Science **289**, 422 (2000).
[3] H. J. Hug, M. A. Lantz, A. Abdurixit, P. J. A. van Schendel, R. Hoffmann, P. Kappenberger, and A. Baratoff, Science **291**, 2509a (2001).
[4] P. Ebert, B. Engels, P. Richard, K. Schroeder, S. Blügel, C. Domke, M. Heinrich, and K. Urban, Phys. Rev. Lett. **77**, 2997 (1996).
[5] R. J. Hamers, R. M. Tromp and J. E. Demuth, Phys. Rev. Lett. **56**, 1972 (1986).
[6] J. A. Stroscio, R. M. Feenstra, and A. P. Fein, Phys. Rev. Lett. **57**, 2579 (1986).
[7] K. C. Pandey, Phys. Rev. Lett. **47**, 1913 (1981).
[8] Any tip modification can be detected by a sudden change from one scan line in the image to the next one.
[9] M. Rohlfing, M. Palummo, G. Onida, and R. Del Sole, Phys. Rev. Lett. **85**, 5440 (2000).
[10] A. A. Stekolnikov, J. Furthmüller, and F. Bechstedt, Phys. Rev. B **65**, 115318 (2002).
[11] M. Rohlfing, and S. G. Louie, Phys. Rev. Lett. **83**, 856 (1999).
[12] R. I. G. Uhrberg, G. V. Hansson, J. M. Nicholls, and S. A. Flodström, Phys. Rev. Lett. **48**, 1032 (1982).
[13] P. Perfetti, J. M. Nicholls, and B. Reihl, Phys. Rev. B **36**, 6160 (1987).
[14] C. Bracher, W. Becker, S. A. Gurvitz, M. Kleber, and M. S.

Marinov, Am. J. Phys. **66**, 38 (1998).
[15] R. M. Feenstra and J. A. Stroscio, J. Vac. Sci. Technol. B **5**, 923 (1987).
[16] F. J. Himpsel, G. Hollinger, and R. A. Pollak, Phys. Rev. B **28**, 7014 (1983).
[17] V. A. Ukraintsev, Phys. Rev. B **53**, 11176 (1996).